



REGULAR ARTICLE

Synthesis, evaluation and *in silico* studies of novel BRD4 bromodomain inhibitors bearing a benzo[*d*]isoxazol scaffold

MAOFENG ZHANG^{a,b,*} , ZHUYUN LIU^a, LIZHONG WANG^{a,b}, YAN LI^a and YONGGANG MA^a

^aCollege of Pharmacy, Taizhou Polytechnic College, Taizhou 225300, People's Republic of China

^bJiangsu Solid Preparation Engineering Technology Research and Development Center, Taizhou 225300, People's Republic of China

E-mail: zhang_maofeng@163.com

MS received 7 May 2020; revised 16 September 2020; accepted 8 November 2020

Abstract. The BRD4 protein is associated with various diseases, which has been an attractive target for the treatment of cancer and inflammation. This paper is a follow-up to our previous studies, in which we report the structure-based design, synthesis, and evaluation of a new class of small-molecule BRD4 bromodomain inhibitors bearing a benzo[*d*]isoxazol scaffold. The SARs focused on exploration of the 2' or 3' position to afford novel inhibitors that may avoid potential metabolically unstable site. The most potent inhibitor **13f** exhibited high binding affinity to BRD4(1) with a ΔT_m value of 7.8 °C as evaluated in thermal shift assay (TSA). The potent activity was also demonstrated by a peptide competition assay with an IC_{50} value of 0.21 μ M. The docking studies revealed the binding mode of the compounds with the active site of BRD4(1). In addition, *in silico* predictions indicated that these compounds possessed good drug-likeness and pharmacokinetic profile.

Keywords. Benzo[*d*]isoxazol; BRD4; bromodomain; molecular docking.

1. Introduction

Acetylation of histone is a classical post-translational modification in the field of epigenetics, which plays an important role in the regulation of chromatin structure. ϵ -N-acetylation of lysine residues on the amino-terminal tails of histones was discovered 30 years ago and has been associated with the opening of chromatin architecture.¹ The opened structure can be accessed by DNA and RNA polymerases as well as transcription factors, resulting in the activation of gene transcription. Acetylation level on histones is highly regulated by histone acetyltransferases (HATs; enzymes that produce or write acetylation marks) and histone deacetylases (HDACs; enzymes that erase acetylation marks), wherein bromodomains act as readers of the acetyl lysine to participate in this regulation process.^{2,3}

The human proteome encodes 61 bromodomains, which are existed in 46 diverse nuclear and

cytoplasmic proteins. These bromodomains can be phylogenetically divided into eight distinct families.⁴ The BET family consists of BRD2, BRD3, BRD4, and BRDT. These proteins bind to the acetylated lysine via their tandem BD1 (expressed as BRD4(1)) and BD2 (expressed as BRD4(2)) domains. The BRD4 protein has been associated with several human diseases and conditions including cancers such as acute myeloid leukemia (AML),^{5,6} MLL,⁷ gastrointestinal stromal tumor (GIST),⁸ triple-negative breast cancer,^{9,10} prostate cancer,^{11–13} neuroblastoma,¹⁴ pancreatic cancer,¹⁵ cholangiocarcinoma,¹⁶ as well as inflammations.^{17–19}

The first BRD4 bromodomain inhibitor was a triazolobenzodiazepine derivative named as (+)-JQ1 (**1**). This compound has been widely used as a probe for exploring the function of BET inhibition.²⁰ Another triazolobenzodiazepine derivative GSK525762 (I-BET762) was reported by Nicodeme *et al.* (Figure 1),¹⁸ which has entered clinical trials for

*For correspondence

Supplementary Information: The online version of this article (<https://doi.org/10.1007/s12039-020-01874-2>) contains supplementary material, which is available to authorized users.

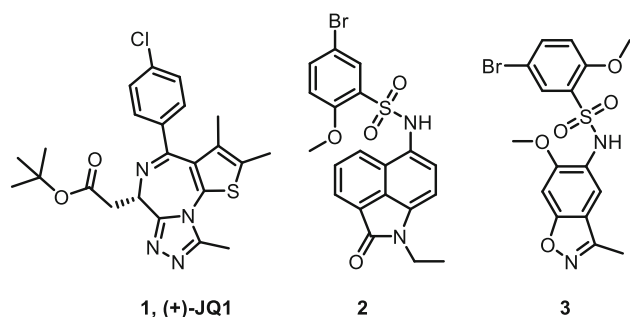


Figure 1. Representative BRD4 bromodomain inhibitors.

neoplasms.^{21,22} The second class were 3,5-dimethylisoxazole containing BRD4 inhibitors such as I-BET151.²³ The 3,5-dimethylisoxazole was an effective warhead and has been introduced to different BET inhibitors.^{24–26} We previously reported the design of a class of inhibitors containing a benzo[*cd*]indol-2(1*H*)-one scaffold, as exemplified by compound **2**,²⁷ and a class of inhibitors containing a benzo[*d*]isoxazol scaffold, as exemplified by compound **3** (Figure 1).²⁸ Compounds **3** demonstrated good therapeutic effects in a C4-2B prostate cancer xenograft tumor model in mice.²⁸ In this paper, we aimed to extend the SAR studies on the 2' and 3' position of compound **3**, and a series of new compounds was designed, synthesized and evaluated as BRD4(1) inhibitors.

2. Experimental

2.1 General chemistry

Melting points were recorded on X-6 melting point apparatus (Beijing Tech instrument, Beijing, China). TLC analysis was performed on GF254 pre-coated silica gel plate (Qingdao Haiyang Chemical, Qingdao, China) and visualized with UV light. ¹H and ¹³C nuclear magnetic resonance (NMR) spectroscopy was performed on a Bruker AV-400 or AV-500 instrument (Bruker, Fällanden, Switzerland) with DMSO-*d*₆ or CDCl₃ as the solvent. Tetramethylsilane (TMS) was used as an internal standard. The coupling constants (*J*) are expressed in hertz (Hz), the chemical shifts (δ) are reported in parts per million (ppm). Signal multiplicities are represented as singlet (s), broad singlet (brs), doublet (d), dd (double doublet), triplet (t), and multiplet (m). The ESI-MS were recorded on an Agilent 1200 HPLC-MSD mass spectrometer (Agilent, California, USA). All solvents and reagents were commercially available and used without further purification.

2.2 General procedures for the preparation of intermediates **9** and **12a–e**

2.2a Ethyl 2-(4-bromo-2-(chlorosulfonyl)phenoxy)acetate (12c): Step 1: Synthesis of ethyl 2-(4-bromophenoxy)acetate (11c). To a solution of 4-bromophenol (**10a**) (3.0 g, 17.34 mmol) in DMF (10 mL) was added K₂CO₃ (7.19 g, 52.02 mmol) followed by the addition of ethyl chloroacetate (2.55 g, 20.81 mmol). The mixture was stirred at 80 °C for 4 h. After the reaction was completed (monitored by TLC), water was added to the mixture. The precipitated solid was filtered and dried to give the title compound as a white solid. Yield: 99%. ¹H NMR (CDCl₃, 400 MHz), δ 7.39 (d, 2H, *J* = 9.0 Hz, 3', 5'-ArH), 6.80 (d, 2H, *J* = 9.0 Hz, 2', 6'-ArH), 4.59 (s, 2H, -OCH₂CO-), 4.27 (q, 2H, *J* = 7.0 Hz, -COOCH₂-), 1.30 (t, 3H, *J* = 7.3 Hz, -CH₂CH₃); ESI-MS (*m/z*): 283.3 [M + Na]⁺. **Step 2: Synthesis of ethyl 2-(4-bromo-2-(chlorosulfonyl)phenoxy)acetate (12c).** To an ice-cooled solution of compound **11c** (400 mg, 1.54 mmol) in CH₂Cl₂ (2 mL) was added a solution of chlorosulfonic acid (1.08 g, 9.26 mmol) in CH₂Cl₂ (4 mL) over a period of 2 min. The reaction was stirred at room temperature for 45 min. Thionyl chloride (2.39 g, 20.07 mmol) was added slowly to the reaction and stirred for additional 3.5 h. After the reaction was completed (monitored by TLC), the mixture was poured into ice-water and extracted with ethyl acetate. The organic layer was washed with water, dried over Na₂SO₄ and concentrated under reduced pressure to give the title compound as a white solid. Yield: 82%. M.p. 124–126 °C; ¹H NMR (CDCl₃, 400 MHz) δ 8.11 (d, 1H, *J* = 2.4 Hz, 3'-ArH), 7.74 (dd, 1H, *J* = 8.9, 2.4 Hz, 5'-ArH), 6.88 (d, 1H, *J* = 8.9 Hz, 6'-ArH), 4.86 (s, 2H, -OCH₂CO-), 4.28 (q, 2H, *J* = 7.1 Hz, -OCH₂CH₃), 1.29 (t, 3H, *J* = 7.1 Hz, -CH₂CH₃); ¹³C NMR (126 MHz, CDCl₃) δ 167.20, 154.78, 139.66, 133.60, 132.44, 115.85, 113.42, 66.33, 62.15, 14.24; ESI-MS (*m/z*): 380.9 [M + Na]⁺.

2.2b 5-Bromo-2,3-dihydrobenzofuran-7-sulfonyl chloride (12e): To an ice-cooled solution of compound **11d** (400 mg, 2.01 mmol) in CH₂Cl₂ (2 mL) was added a solution of chlorosulfonic acid (1.4 g, 12.06 mmol) in CH₂Cl₂ (4 mL) over a period of 2 min. The reaction was stirred at room temperature for 2.5 h. On completion of the reaction, the mixture was poured into ice water and the CH₂Cl₂ was evaporated under reduced pressure. The precipitated solid was filtered and dried to give the target compound as a white solid. Yield: 75%. M.p. 123–124 °C. ¹H NMR (400 MHz, CDCl₃) δ

7.81–7.74 (m, 1H, ArH), 7.60 (d, $J = 1.7$ Hz, 1H, ArH), 4.91 (t, $J = 8.8$ Hz, 2H, $-\text{OCH}_2\text{CH}_2-$), 3.35 (t, $J = 8.8$ Hz, 2H, $-\text{CH}_2\text{CH}_2\text{Ar}$); ^{13}C NMR (126 MHz, CDCl_3) δ 156.82, 135.08, 134.02, 128.72, 126.88, 111.89, 74.58, 28.94; ESI-MS (m/z): 321.0 $[\text{M} + \text{Na}]^+$.

The procedures for the preparation of intermediates **9**, **11d**, **12a–b** and **12d** were described in supplementary information.

2.3 General procedures for the preparation of compounds **13a–h**

2.3a 5-Bromo-2-ethoxy-*N*-(6-methoxy-3-methylbenzo[d]isoxazol-5-yl)benzenesulfonamide (13a): To a solution of compound **9** (100 mg, 0.56 mmol) in CH_2Cl_2 (6 mL) was added 5-bromo-2-ethoxybenzenesulfonyl chloride (184.9 mg, 0.62 mmol) followed by the addition of pyridine (0.3 mL). The resulting mixture was stirred at 43 °C for 3 h. Upon completion of the reaction (monitored by TLC, ethyl acetate/light petroleum (1:1, v/v)), the mixture was cooled and diluted with 1 mol/L HCl (8 mL) and water (12 mL), which was then extracted with ethyl acetate (3 \times 20 mL). The organic layer was washed successively with water and brine, dried over Na_2SO_4 and concentrated under reduced pressure. The residue was purified by silica gel chromatography to give the title compound as a white solid. Yield: 65%. M.p. 173–174 °C; ^1H NMR (400 MHz, CDCl_3) δ 7.95 (d, $J = 2.5$ Hz, 1H, 6'-ArH), 7.71 (s, 1H, 7-ArH), 7.58–7.50 (m, 2H, 4'-ArH, $-\text{NH}-$), 6.90 (s, 1H, 4-ArH), 6.83 (d, $J = 8.8$ Hz, 1H, 3'-ArH), 4.18 (q, $J = 7.0$ Hz, 2H, $-\text{CH}_2-$), 3.83 (s, 3H, 6-OCH₃), 2.52 (s, 3H, 3-CH₃), 1.56 (t, $J = 7.0$ Hz, 3H, $-\text{CH}_2\text{CH}_3$); ^{13}C NMR (101 MHz, CDCl_3) δ 160.89, 155.21, 155.02, 152.28, 137.49, 133.05, 128.42, 123.38, 115.17, 114.44, 112.38, 112.18, 91.92, 65.33, 56.28, 14.58, 10.07; ESI-MS (m/z): 441.0 and 443.0 $[\text{M} + \text{H}]^+$.

2.3b 5-Bromo-2-hydroxy-*N*-(6-methoxy-3-methylbenzo[d]isoxazol-5-yl)benzenesulfonamide (13b): White solid. Yield: 66%. M.p. 202–203 °C; ^1H NMR (400 MHz, CDCl_3) δ 7.69 (s, 1H, 7-ArH), 7.57 (d, $J = 2.4$ Hz, 1H, 6'-ArH), 7.45 (dd, $J = 8.9$, 2.4 Hz, 1H, 4'-ArH), 6.87 (s, 1H, 4-ArH), 6.78 (d, $J = 8.9$ Hz, 1H, 3'-ArH), 3.69 (s, 3H, 6-OCH₃), 2.55 (s, 3H, 3-CH₃); ^{13}C NMR (101 MHz, DMSO) δ 161.48, 155.73, 155.06, 154.94, 136.79, 130.88, 127.82, 123.13, 119.35, 117.90, 114.08, 108.60, 92.38, 56.19, 9.46; ESI-MS (m/z): 412.9 and 414.9 $[\text{M} + \text{H}]^+$.

2.3c 5-Bromo-*N*-(6-methoxy-3-methylbenzo[d]isoxazol-5-yl)-2-(trifluoromethoxy)benzene sulfonamide (13c): White solid. Yield: 66%. M.p. 165–166 °C; ^1H NMR (500 MHz, CDCl_3) δ 8.04 (d, $J = 2.4$ Hz, 1H, 6'-ArH), 7.72 (s, 1H, 7-ArH), 7.66 (dd, $J = 8.8$, 2.4 Hz, 1H, 4'-ArH), 7.30 (brs, 1H, $-\text{NH}-$), 7.21 (dd, $J = 8.8$, 1.7 Hz, 1H, 3'-ArH), 6.90 (s, 1H, 4-ArH), 3.81 (s, 3H, 6-OCH₃), 2.53 (s, 3H, 3-CH₃); ^{13}C NMR (101 MHz, CDCl_3) δ 161.48, 155.21, 152.77, 145.22, 137.60, 134.11, 132.11, 124.05 ($-\text{OCF}_3$), 122.15, 121.45 ($-\text{OCF}_3$), 120.61 ($-\text{ArCOCF}_3$), 120.59 ($-\text{ArCOCF}_3$), 120.57 ($-\text{ArCOCF}_3$), 120.55 ($-\text{ArCOCF}_3$), 119.08, 118.84 ($-\text{OCF}_3$), 116.24 ($-\text{OCF}_3$), 115.20, 113.88, 91.99, 56.21, 10.05; ESI-MS (m/z): 480.9 and 482.9 $[\text{M} + \text{H}]^+$.

2.3d 5-Bromo-*N*-(6-methoxy-3-methylbenzo[d]isoxazol-5-yl)-2-propoxybenzenesulfonamide (13d): White solid. Yield: 67%. M.p. 159–160 °C; ^1H NMR (400 MHz, CDCl_3) δ 7.93 (d, $J = 2.4$ Hz, 1H, 6'-ArH), 7.71 (s, 1H, 7-ArH), 7.54 (dd, $J = 8.8$, 2.4 Hz, 1H, 4'-ArH), 7.49 (brs, 1H, $-\text{NH}-$), 6.89 (s, 1H, 4-ArH), 6.84 (d, $J = 8.8$ Hz, 1H, 3'-ArH), 4.07 (t, $J = 6.5$ Hz, 2H, $-\text{OCH}_2\text{CH}_2-$), 3.81 (s, 3H, 6-OCH₃), 2.52 (s, 3H, 3-CH₃), 2.02–1.87 (m, 2H, $-\text{CH}_2\text{CH}_2-$), 1.15 (t, $J = 7.4$ Hz, 3H, $-\text{CH}_2\text{CH}_3$); ^{13}C NMR (101 MHz, DMSO) δ 161.49, 155.55, 155.49, 154.96, 137.04, 131.30, 129.67, 123.01, 117.96, 115.73, 114.14, 110.27, 92.36, 70.43, 56.31, 21.49, 10.29, 9.46; ESI-MS (m/z): 455.0 and 457.0 $[\text{M} + \text{H}]^+$.

2.3e Ethyl 2-(4-bromo-2-(*N*-(6-methoxy-3-methylbenzo[d]isoxazol-5-yl)sulfamoyl)phenoxy)acetate (13e): White solid. Yield: 69%. M.p. 174–176 °C; ^1H NMR (400 MHz, CDCl_3) δ 8.11 (s, 1H, $-\text{NH}-$), 7.93 (d, $J = 2.5$ Hz, 1H, 6'-ArH), 7.73 (s, 1H, 7-ArH), 7.57 (dd, $J = 8.7$, 2.5 Hz, 1H, 4'-ArH), 6.87 (s, 1H, 4-ArH), 6.78 (d, $J = 8.8$ Hz, 1H, 3'-ArH), 4.73 (s, 2H, $-\text{OCH}_2\text{CO}-$), 4.32 (q, $J = 7.1$ Hz, 2H, $-\text{OCH}_2\text{CH}_3$), 3.71 (s, 3H, 6-OCH₃), 2.53 (s, 3H, 3-CH₃), 1.33 (t, $J = 7.1$ Hz, 3H, $-\text{OCH}_2\text{CH}_3$); ^{13}C NMR (101 MHz, CDCl_3) δ 167.50, 161.43, 155.18, 153.92, 153.63, 137.18, 132.81, 130.31, 123.00, 115.18, 115.16, 115.06, 113.80, 91.93, 66.49, 62.11, 56.16, 14.15, 10.04; ESI-MS (m/z): 499.0 and 501.0 $[\text{M} + \text{H}]^+$.

2.3f 5-Bromo-*N*-(6-methoxy-3-methylbenzo[d]isoxazol-5-yl)-2,3-dihydrobenzofuran-7-sulfonamide (13f): White solid. Yield: 74%. M.p. 189–190 °C; ^1H NMR (400 MHz, CDCl_3) δ 7.69 (s,

1H, 7-ArH), 7.64 (s, 1H, 6'-ArH), 7.46–7.32 (m, 2H, 4'-ArH, -NH-), 6.90 (s, 1H, 4-ArH), 4.71 (t, $J = 8.8$ Hz, 2H, -OCH₂-), 3.84 (s, 3H, 6-OCH₃), 3.22 (t, $J = 8.7$ Hz, 2H, -CH₂Ar-), 2.52 (s, 3H, 3-CH₃); ¹³C NMR (101 MHz, CDCl₃) δ 161.04, 156.13, 155.21, 152.45, 132.83, 131.95, 130.01, 123.13, 121.96, 115.08, 112.51, 111.72, 91.88, 73.58, 56.37, 28.90, 10.06; ESI-MS (m/z): 439.0 and 441.0 [M + H]⁺.

2.3g *N*-(6-methoxy-3-methylbenzo[d]isoxazol-5-yl)benzo[c][1, 2, 5]thiadiazole-4-sulfonamide (**13g**): White solid. Yield: 69%. M.p. 230–231 °C; ¹H NMR (400 MHz, DMSO) δ 9.76 (s, 1H, -NH-), 8.37 (d, $J = 8.7$ Hz, 1H, 7'-ArH), 7.99 (d, $J = 7.0$ Hz, 1H, 5'-ArH), 7.75 (t, $J = 8.0$ Hz, 1H, 6'-ArH), 7.71 (s, 1H, 7-ArH), 7.04 (s, 1H, 4-ArH), 2.96 (s, 3H, 6-OCH₃), 2.50 (s, 3H, 3-CH₃); ¹³C NMR (101 MHz, DMSO) δ 162.01, 156.52, 155.05, 154.96, 149.10, 131.92, 130.73, 128.66, 126.15, 122.30, 120.85, 114.28, 92.11, 55.44, 9.50; ESI-MS (m/z): 377.0 [M + H]⁺.

2.3h *N*-(6-methoxy-3-methylbenzo[d]isoxazol-5-yl)quinoline-8-sulfonamide (**13h**): White solid. Yield: 70%. M.p. 212–213 °C; ¹H NMR (500 MHz, DMSO) δ 9.17 (m, 1H, 2'-ArH), 9.10 (brs, 1H, -NH-), 8.56 (d, $J = 8.3$ Hz, 1H, 7'-ArH), 8.28 (d, $J = 8.3$ Hz, 1H, 5'-ArH), 8.21 (d, $J = 7.2$ Hz, 1H, 4'-ArH), 7.80–7.75 (m, 1H, 6'-ArH), 7.73 (s, 1H, 7-ArH), 7.65 (t, $J = 7.7$ Hz, 1H, 3'-ArH), 7.07 (s, 1H, 4-ArH), 3.21 (s, 3H, 6-OCH₃), 2.46 (s, 3H, 3-CH₃); ¹³C NMR (101 MHz, DMSO) δ 160.91, 154.91, 154.16, 151.23, 142.66, 137.08, 135.68, 134.11, 130.66, 128.44, 125.47, 123.59, 122.66, 115.62, 114.13, 92.28, 55.77, 9.45; ESI-MS (m/z): 370.0 [M + H]⁺.

2.4 General procedures for the preparation of compounds **14**, **14a–c**

2.4a *2*-(4-Bromo-2-(*N*-(6-methoxy-3-methylbenzo[d]isoxazol-5-yl)sulfamoyl)phenoxy)acetic acid (**14**): To a solution of 2 mol/L NaOH (12 mL) was added compound **13e** (500 mg, 1.0 mmol). The mixture was stirred at room temperature for 4 h. On completion of the reaction (monitored by TLC), the mixture was treated with 1 mol/L dilute hydrochloric acid to adjust the pH value to 5–6. The precipitated solid was filtered to obtain the target compound as a white solid. Yield: 98%. M.p. 204–205 °C; ¹H NMR (400 MHz, DMSO-*d*₆) δ 9.25 (brs, 1H, -COOH),

7.76 (dd, $J = 8.9, 2.5$ Hz, 1H, 4'-ArH), 7.66 (s, 1H, 7-ArH), 7.64 (d, $J = 2.5$ Hz, 1H, 6'-ArH), 7.24 (s, 1H, 4-ArH), 7.15 (d, $J = 8.9$ Hz, 1H, 3'-ArH), 4.90 (s, 2H, -OCH₂CO-), 3.63 (s, 3H, 6-OCH₃), 2.46 (s, 3H, 3-CH₃); ¹³C NMR (101 MHz, DMSO) δ 169.92, 161.62, 155.90, 154.99, 154.54, 136.95, 130.74, 129.95, 122.61, 118.83, 116.37, 114.22, 111.34, 92.53, 65.85, 56.36, 9.46; ESI-MS (m/z): 468.9 and 470.9 [M-H]⁻.

2.4b *2*-(4-Bromo-2-(*N*-(6-methoxy-3-methylbenzo[d]isoxazol-5-yl)sulfamoyl)phenoxy)-*N*-methylacetamide (**14a**): To a solution of compound **14** (80 mg, 0.17 mmol) in DMF (5 mL) were added diisopropylethylamine (DIPEA) (76.8 mg, 0.59 mmol) and HATU (96.8 mg, 0.25 mmol). The resulting mixture was stirred at room temperature for 15 min followed by the addition of methylamine hydrochloride (19.5 mg, 0.29 mmol). The mixture was stirred at room temperature for additional 5 h. After the reaction was completed, it was diluted with water (10 mL) and the precipitated solid was filtered. The crude product was purified by silica gel chromatography to obtain the target compound as a white solid. Yield: 75%. M.p. 183–184 °C; ¹H NMR (400 MHz, CDCl₃) δ 7.84 (d, $J = 2.4$ Hz, 1H, 6'-ArH), 7.70 (s, 1H, 7-ArH), 7.59 (dd, $J = 8.8, 2.4$ Hz, 1H, 4'-ArH), 7.44 (brs, 1H, -CONH-), 7.34 (s, 1H, -SO₂NH-), 6.87 (s, 1H, 4-ArH), 6.85 (d, $J = 8.9$ Hz, 1H, 3'-ArH), 4.64 (s, 2H, -OCH₂CO-), 3.73 (s, 3H, 6-OCH₃), 2.90 (d, $J = 4.8$ Hz, 3H, -NHCH₃), 2.53 (s, 3H, 3-CH₃); ¹³C NMR (101 MHz, CDCl₃) δ 167.34, 161.57, 155.16, 153.43, 153.08, 137.96, 133.29, 128.57, 122.26, 115.30, 115.04, 114.34, 113.79, 92.06, 67.94, 56.43, 26.10, 10.04; ESI-MS (m/z): 484.0 and 486.0 [M + H]⁺.

2.4c *2*-(4-Bromo-2-(*N*-(6-methoxy-3-methylbenzo[d]isoxazol-5-yl)sulfamoyl)phenoxy)-*N*-ethylacetamide (**14b**): White solid. Yield: 70%. M.p. 195–196 °C; ¹H NMR (400 MHz, CDCl₃) δ 7.85 (d, $J = 2.4$ Hz, 1H, 6'-ArH), 7.70 (s, 1H, 7-ArH), 7.59 (dd, $J = 8.8, 2.4$ Hz, 1H, 4'-ArH), 7.44 (s, 1H, -CONH-), 7.33 (s, 1H, -SO₂NH-), 6.87 (s, 1H, 4-ArH), 6.84 (d, $J = 8.8$ Hz, 1H, 3'-ArH), 4.63 (s, 2H, -OCH₂CO-), 3.74 (s, 3H, 6-OCH₃), 3.43–3.34 (m, 2H, -CH₂CH₃), 2.53 (s, 3H, 3-CH₃), 1.21 (t, $J = 7.3$ Hz, 3H, -CH₂CH₃); ¹³C NMR (101 MHz, CDCl₃) δ 166.40, 161.52, 155.16, 153.42, 152.95, 137.94, 133.30, 128.55, 122.33, 115.31, 114.76, 114.32, 113.75, 92.06, 67.93, 56.45, 34.34, 14.50, 10.06; ESI-MS (m/z): 498.0 and 500.0 [M + H]⁺.

2.4d 2-(4-Bromo-2-(N-(6-methoxy-3-methylbenzo[d]isoxazol-5-yl)sulfamoyl)phenoxy)-N-propylacetamide (**14c**): White solid. Yield: 65%. M.p. 180–181 °C; ^1H NMR (400 MHz, CDCl_3) δ 7.85 (d, $J = 2.4$ Hz, 1H, 6'-ArH), 7.70 (s, 1H, 7-ArH), 7.59 (dd, $J = 8.8, 2.4$ Hz, 1H, 4'-ArH), 7.44 (s, 1H, -CONH-), 7.32 (s, 1H, -SO₂NH-), 6.87 (s, 1H, 4-ArH), 6.85 (d, $J = 8.8$ Hz, 1H, 3'-ArH), 4.64 (s, 2H, -OCH₂CO-), 3.75 (s, 3H, 6-OCH₃), 3.31 (q, $J = 6.8$ Hz, 2H, -NHCH₂CH₂-), 2.53 (s, 3H, 3-CH₃), 1.65–1.54 (m, 2H, -CH₂CH₂CH₃), 0.94 (t, $J = 7.4$ Hz, 3H, -CH₂CH₃); ^{13}C NMR (101 MHz, CDCl_3) δ 166.51, 161.50, 155.16, 153.39, 152.90, 137.94, 133.30, 128.53, 122.35, 115.31, 114.64, 114.29, 113.76, 92.07, 67.90, 56.45, 41.16, 22.56, 11.37, 10.06; ESI-MS (m/z): 512.0 and 514.0 [$\text{M} + \text{H}$]⁺.

2.5 Docking studies

Preparation of the Receptor. The protein of compound **3** in complex with BRD4(1) (PDB ID: 5Y8Y) was utilized for generation of grid. The protein was prepared using the Protein Preparation Wizard within Maestro (version 11.5, implanted in Schrödinger). The bond orders were assigned using CCD database, the hydrogens were added, and the missing side chains were filled in with Prime. The original waters beyond 5.0 Å from ligand were deleted. In addition, the solvent water molecules near the 6-OCH₃ position were also deleted. The important inner water molecules were kept. The states of ligands were generated using Epik and the pH value was set as 7.0 ± 2.0. The water orientations were optimized via the H-bond assignment using PROPKA program and the pH value was set as 7.0. OPLS3 force field was used to minimize the energy of the added hydrogens.

Preparation of the Ligands. The ligands were prepared using the LigPrep program with default parameters. The energy minimization was performed using an OPLS3 force field.

Individual Docking. The docking studies were carried out using the Ligand Docking module. The grid was defined similar in size to the original ligand. No constraints were applied, and all parameters were kept as default. The compounds were docked using Glide SP mode.

2.6 Biochemical assays

2.6a Protein expression and purification: The expression and purification of BRD4 BD1 proteins

were carried out as previously described.^{27,28} The experimental detail was described in supplementary information.

2.6b Thermal shift assay (T_m): Thermal shift assays were performed using the Bio-Rad CFX96 Real-Time PCR system. Each biochemical reaction consists 10 μM protein, 200 μM compound, a fluorescent dye (SYPRO Orange, ABI, Sigma) that was added at a dilution of 1:1000, and a buffer (10 mM HEPES, 150 mM NaCl, 50% (v / v) glycerin as well as deionized water at a pH of 7.5). The reaction mixture (20 μL) was added to the 96-well plate. Next, the mixture was centrifuged at 1000 r/min for 1 min at room temperature and incubated on ice for 30 min in the dark. The excitation and emission filters of the SYPRO Orange dye were set at 465 nm and 590 nm, respectively. Raising the temperature from 30 °C to 80 °C at a rate of 0.3 °C/min. The signal of fluorescence was read at an interval of 0.3 °C. All experiments were performed in triplicate. The melting temperature (T_m) was calculated by fitting the melting curve to Boltzmann equation using GraphPad Prism. ΔT_m represents the difference between the calculated T_m values for the tested reaction and the blank reaction.

2.6c AlphaScreen peptide displacement assay: The interaction between the protein of BRD4 BD1 bromodomain and ligand was evaluated by AlphaScreen technique (PerkinElmer). The biochemical reaction consisted of 50 nM protein, 50 nM peptide, the indicated concentration of compounds, deionized water, and the buffer (50 mM MOPS, 0.05 mM CHAPS, 50 mM NaF, 0.1 mg/mL BSA and deionized water at a pH value of 7.4). All components were mixed in a 384-well plate (ProxiPlate-384 Plus, PerkinElmer, USA) for 1 h at room temperature. The nickel receptor beads and streptavidin donor beads were dilute with buffer to indicated concentration, and were added to the above 384-well plate at a final concentration of 5 μg/mL in the dark environment. The plates were sealed with foil to avoid light and incubated for 1.5 h at room temperature. The signal was read on an EnSpire microplate reader (PerkinElmer, USA). The protein of BRD4 bromodomain binds to the nickel acceptor beads. The biotinylated acetylated histone H4 peptide binds to streptavidin donor beads. When the donor beads were excited by a 680 nm laser beam, it will emit $^1\text{O}_2$. The $^1\text{O}_2$ can activate the acceptor beads to release 520 nm photons as signals. All experiments were performed on the same plate in triplicate. The peptide used above is a C-terminal biotinylated tetra-

acetylated histone peptide (bH4KAc4) with the sequence of H-YSGRGK(Ac)GGK(Ac)GLGK(Ac)GGAK(Ac)RHRK-Biotin-OH (synthesized by Genscript). The inhibitory curves (Figure S1, Supplementary Information) and half-maximal inhibitory concentration (IC_{50}) values were calculated using GraphPad Prism 7 software. The raw data read from the microplate reader was firstly transformed to logarithms, and then analyzed using the nonlinear regression of curve fit. The dose-response inhibition equation was chosen to generate the presented curves and IC_{50} values.

3. Results and Discussion

3.1 Chemistry

The benzo[*d*]isoxazol containing scaffold **9** can be synthesized *via* multistep reactions from commercially available 2, 4-dimethoxyaniline (**4**).²⁸ As outlined in Scheme 1, the amino group of **4** was protected with acetic anhydride to give compound **5**, which could be converted to compound **6** via a Friedel-Crafts reaction in the presence of a lewis acid of $AlCl_3$. Next, the ketone group of **6** was reacted with hydroxylamine hydrochloride, which afforded the oxime product **7**. Compound **7** could undergo a cyclization in the presence of DMF-DMA under high temperature to afford the benzo[*d*]isoxazol scaffold **8**. Finally, the acetyl group of **8** was hydrolyzed by hydrochloric acid to give the aniline **9**.

The synthesis of different sulfonyl chlorides was described in Scheme 2. The commercially available 4-bromophenol (**10a**) was reacted with different haloalkanes to give the intermediates **11a–c**. Treatment of **10a** or **11a–c** with chlorosulfonic acid gave

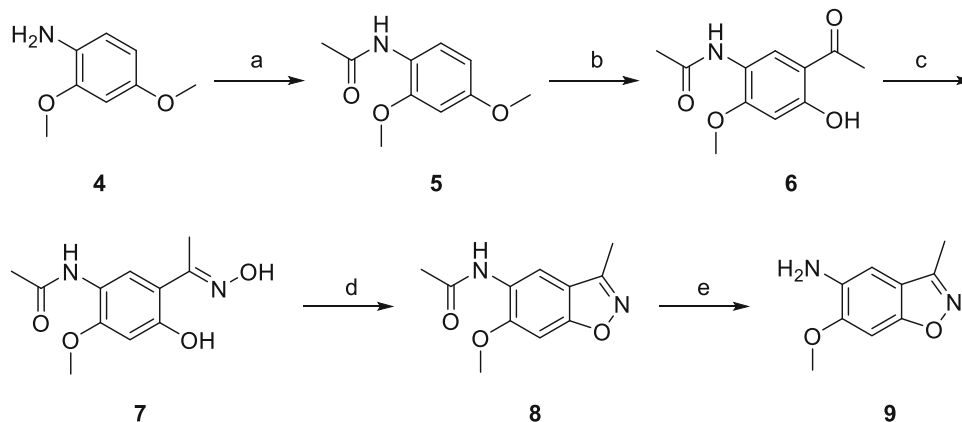
the sulfonyl chlorides **12a–d**. The 5-bromo-2, 3-dihydrobenzofuran-7-sulfonyl chloride (**12e**) was prepared using the 2, 3-dihydrobenzofuran (**10b**) as the starting material. The compound **10b** was treated with Br_2 to afford the bromine substituted intermediate **11d**,²⁹ followed by the treatment of chlorosulfonic acid to generate target intermediate **12e**.

Finally, the scaffold of **9** was reacted with various sulfonyl chlorides in a one-plot procedure to obtain the target compounds **13a–h** (Scheme 3). Hydrolysis of **13e** with NaOH solution afforded compound **14**, which was coupled with available amines to generate the target compounds **14a–c** (Scheme 3).

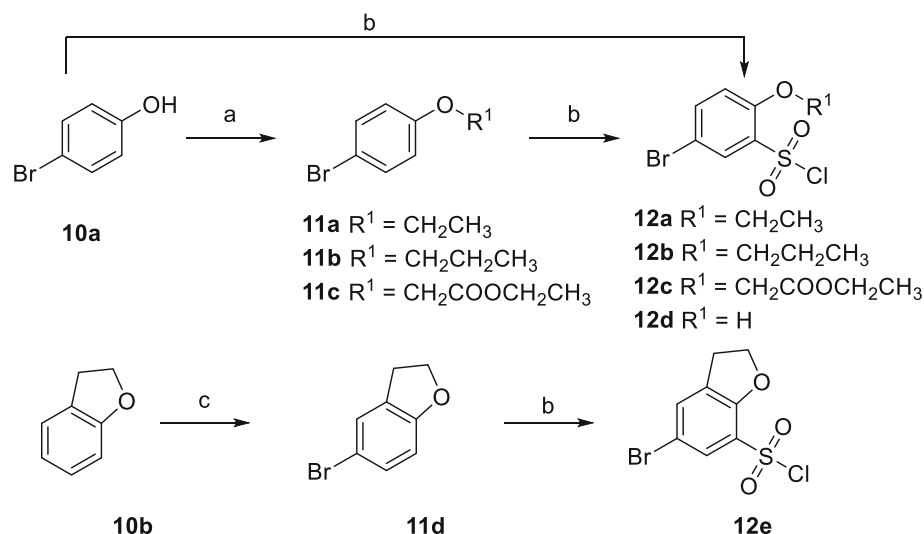
3.2 SARs studies

This work began with an analysis of the co-crystal structure of **3**-BRD4(1) complex as reported in our previous work.²⁸ According to the structural analysis, the 3-methylbenzo[*d*]isoxazole scaffold resided in the binding pocket and formed direct or indirect hydrogen bonds with key residues (Figure 2). It is obvious that 2'-methoxy of compound **3** extends to the solvent region, which guarantees the chemical space for modification. The CYP-mediated O-demethylation is a prevalent metabolic pathway for many drugs.^{30,31} Thus, the methoxy group is a potential metabolic group in the body. The replacement of 2'-methoxy may improve the metabolic stability of compounds (Figure 2). This article aims to test the feasibility of modification on 2' or 3' position, which will extend the structure-activity relationships (SARs).

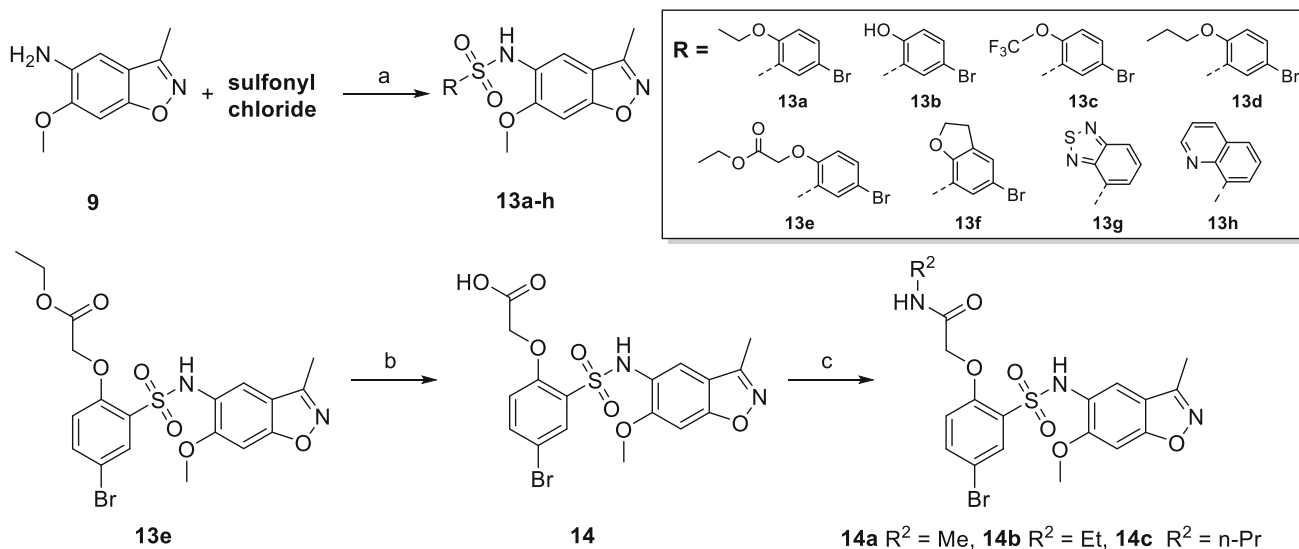
We preliminarily sought to evaluate whether the length of the alkyl chain affects the binding affinity. When an ethyl group was introduced at R¹ position, the resulting compound **13a** exhibited potent binding



Scheme 1. The synthetic route of the benzo[*d*]isoxazol scaffold. Reagents and conditions: (a) Ac_2O , Et_3N , CH_2Cl_2 , rt, 81%; (b) Acetyl chloride, $AlCl_3$, CH_2Cl_2 , 0–43 °C, 82%; (c) $NH_2-OH \cdot HCl$, NaOAc, EtOH/ H_2O , 80 °C, 83%; (d) DMF-DMA, 1,4-dioxane, 100 °C, 66%; (e) HCl/H_2O , 90 °C, 95%.



Scheme 2. The synthetic route of intermediates of sulfonyl chlorides. Reagents and conditions: (a) R^1X ($\text{X} = \text{I}, \text{Br}, \text{Cl}$), K_2CO_3 , DMF, 80°C , 90–99%; (b) ClSO_3H , CH_2Cl_2 , $0^\circ\text{C} - \text{rt}$ (exception, for **12c**: ClSO_3H , CH_2Cl_2 , $0^\circ\text{C} - \text{rt}$, then SOCl_2 , rt), 35–82%; (c) Br_2 , pyridine, CH_2Cl_2 , rt, 91%.



Scheme 3. The synthetic route of target compounds. Reagents and conditions: (a) RSO_2Cl , pyridine, CH_2Cl_2 , 43°C , 65–74%; (b) NaOH , H_2O , rt, 98%; (c) R^2NH_2 , HATU, DIPEA, DMF, rt, 65–75%.

activity with a thermo shift (ΔT_m) value of 7.2°C and an IC_{50} value of $0.47\ \mu\text{M}$ (Table 1). When shortening the carbon chain, a compound **13b** was obtained. This compound had a higher ΔT_m value of 8.4°C compared with **13a**. However, the IC_{50} value ($1\ \mu\text{M}$) was not corresponding to the ΔT_m value, which may attribute to the poor solubility. It was noted that the introduction of a trifluoromethyl group (compound **13c**) at R^1 position led to a 2-fold decrease in potency compared with **13a**. The local steric hindrance produced by trifluoromethoxy group may lead to the change of the relative orientation of the aryl ring as well as the decrease on activity. Docking studies also revealed that the scores of **13c** (-6.182 , -6.427 , -60.583)

were significantly worse than that of **13a** (-6.726 , -6.782 , -63.101) (Table S1, Supplementary Information). Next, we continued to extend the carbon chain. Introduction of propyl on R^1 position led to compound **13d**, which restored the activity with a ΔT_m value of 5.7°C and an IC_{50} value of $0.54\ \mu\text{M}$.

Next, we tried to test the feasibility of the introduction of heteroatom-containing chains at R^1 position, which may be suitable for extending to the solvent region of the protein. When the oxygen-linked ethyl acetate group (compound **13e**) was introduced at the R^1 position, the IC_{50} value was still maintained at $0.42\ \mu\text{M}$. However, the compound did not respond well in TSA experiment. Hydrolyzing the ethyl acetate

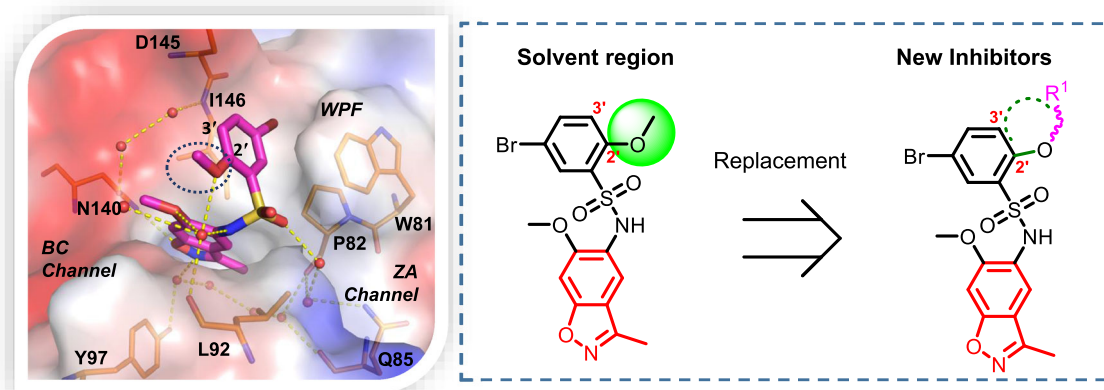


Figure 2. Structure-based design of new BRD4 bromodomain inhibitors.

group of compound **13e** to acetic acid group gave the compound **14**, which exhibited an IC_{50} value of $0.66 \mu\text{M}$ and ΔT_m value of $6.9 \text{ }^\circ\text{C}$ (Table 1). The above results show that R^1 position is tolerated for modifications. Further studies on the exploration of the chemical space of the $2'$ position were carried out. We designed and synthesized several derivatives including methanamide (compound **14a**), acetamide (compound **14b**), propanamide (compound **14c**) substitutions at the $2'$ side chain. All the three compounds displayed high ΔT_m values as evaluated in TSA assay. These compounds also showed submicromole binding activities with the IC_{50} values ranging from $0.35 \mu\text{M}$ to $0.75 \mu\text{M}$. Among the three compounds, **14b** showed stronger activity with IC_{50} value of $0.35 \mu\text{M}$ and ΔT_m value of $7.2 \text{ }^\circ\text{C}$.

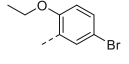
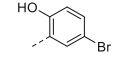
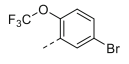
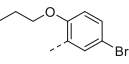
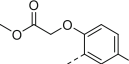
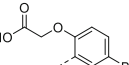
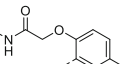
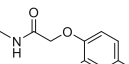
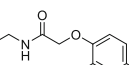
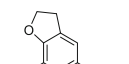
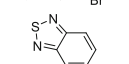
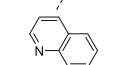
It was noteworthy that most of the above compounds possessed substituents of linear chains. However, the linear chains are flexible, which may lead to unstable conformations. The variable conformations do not benefit binding affinity. Therefore, we designed several compounds with fused rings to immobilize the conformation. According to the crystal structure of **3**-BRD4(1) complex, the $3'$ position was also suitable for small substitution (Figure 2). We also noted that the oxygen atom in $2'$ -methoxy group formed a hydrogen bond with the adjacent water molecule. Therefore, we reserved the oxygen atom at $2'$ position and fused the $2'$ and $3'$ position to afford a new 2, 3-dihydrobenzofuran fragment. The resulting compound **13f** displayed potent binding affinity with a ΔT_m value of $7.8 \text{ }^\circ\text{C}$. The strong activity was also demonstrated by the IC_{50} value of $0.21 \mu\text{M}$, which was only 0.6 fold lower than that of **3** (Table 1). This result met the original expectations to replace the methoxy group with other substituents to avoid potential *in vivo* metabolism

while maintaining the activity with less than 1 fold loss compared with the previous inhibitor **3**. We also synthesized two additional compounds **13g–h** with fused rings. However, both compounds almost lost the binding potencies, probably due to the rigidity and planarity of the fused rings, making it not accommodate in the binding pocket. The data reported here suggest a feasible direction for further chemical modification on the $2'$ position or $3'$ position.

3.3 Molecular docking studies of compounds with BRD4(1)

To understand potential binding interactions of the compounds to BRD4(1), several representative compounds were chosen for molecular docking studies. The crystal structure of **3**-BRD4(1) complex (PDB ID: 5Y8Y) was used for generating the grid. The overall binding mode predicted by molecular docking was shown in Figure 3. The 3-methylbenzo[*d*]isoxazole scaffold of all compounds resided in the binding pocket. The oxygen of isoxazole moiety formed a hydrogen bond with Asn140 (Figure 3A). The nitrogen of isoxazole formed a hydrogen bond with a conserved water molecule, which further bound to Tyr97 (Figure 3A). The 5-bromo-2,3-dihydrobenzofuran fragment of **13f** attached to the sulfonamide could occupy the sub-pocket referred to as the WPF shelf (Figure 3B).²⁵ The Br substituent directed towards Ile146 while the furan ring exposed to the solvent (Figure 3B). The sulfonamide oxygen also formed a hydrogen bond with the nearby water molecule. The representative compounds **13a** and **14b** displayed similar binding mode to that of **13f**.

Table 1. Binding activities of compounds **13a–h**, **14** and **14a–c** against BRD4(1) measured by TSA and AlphaScreen.

No.	R	TSA ΔT_m ($^{\circ}\text{C}$)	AlphaScreen (μM) ^a
13a		7.2	0.47 ± 0.01
13b		8.4	1.04 ± 0.07
13c		NA	1.49 ± 0.17
13d		5.7	0.54 ± 0.04
13e		4.8	0.42 ± 0.03
14		6.9	0.66 ± 0.08
14a		7.0	0.75 ± 0.08
14b		7.2	0.35 ± 0.10
14c		6.6	0.69 ± 0.05
13f		7.8	0.21 ± 0.16
13g		NA	<50% @ 20 μM
13h		NA	<50% @ 20 μM

^aThe IC_{50} of all compounds in the table were calculated from at least two independent experiments. Values are given as the mean \pm SD.

It was noteworthy that the fused 2, 3-dihydrobenzofuran ring exhibited fewer conformations than compounds with long linear chains in the docking process, which may contribute to the improved binding activity. The docking scores of **13a**, **14b**, **13f** and **3** are listed in Table S1 (Supplementary Information). Three kinds of binding energy scores, such as docking score, glide gscore, and glide emodel score, were selected for comprehensive evaluation. Compound **13f** displayed similar docking scores (-6.766 , -6.816 , -61.32) compared with **3** (-6.876 , -6.922 , -62.285). Compounds **13a** (-6.726 , -6.782 , -63.101) and **14b** (-6.358 , -6.407 , -64.341) showed slightly bad scores compared with **13f** and **3**. In summary, the hydrogen bond and hydrophobic

interactions taken together with the good shape complementary contribute to the high binding affinity.

3.4 *In silico studies of drug-likeness and pharmacokinetic profile*

The drug-likeness and pharmacokinetic profile are closely related to the success of drug development. Generally, a qualified clinical candidate often meets some drug-like criteria. Therefore, the representative compounds **13a**, **14b** and **13f** were selected for calculation using the online SwissADME server.³² Firstly, the drug-like profiles of the compounds were analyzed using several classic filters (Table 2). These rules were established based on the basic physicochemical parameters, such as molecular weight (Mw), number of rotatable bonds (NRB), number of the hydrogen-bond acceptor (NHBA), number of hydrogen bond donor (NHBD), topological polar surface area (TPSA) and LogP, which were used to evaluate the chance for a molecule to be an orally available candidate. A summary of the physicochemical parameters of **13a**, **14b** and **13f** was listed in supporting Table S2 (Supplementary Information). Lipinski rule³³ (also known as rule-of-five) is a classic drug-like filter, which can be summarized as the following criteria: $\text{NHBD} \leq 5$, $\text{NHBA} \leq 10$, $\text{LogP} \leq 5$, $\text{NRB} \leq 10$, and $\text{Mw} \leq 500$. Afterwards, several new rules such as Ghose,³⁴ Egan³⁵ Muegge (Bayer)³⁶ and Veber³⁷ rules had been established. The results indicated that only compound **14b** showed 1 violation against the Ghose ruler, other compounds **13a** and **13f** met all of the rules (Table 2). The bioavailability score predicts the probability that a compound will have bioavailability (F) > 10% in rat or measurable Caco-2 permeability.³⁸ For anions, the score is 0.11 when $\text{TPSA} > 150 \text{ \AA}^2$; 0.56 if TPSA between 75 and 150 \AA^2 ; 0.85 if $\text{TPSA} < 75 \text{ \AA}^2$.³⁸ For the rest compounds, the score is 0.55 if it passes the five rules, and 0.17 if it fails.³⁸ All three compounds exhibited promising bioavailability score of 0.55 (Table 2).

The pharmacokinetic profile was predicted using parameters including gastrointestinal absorption (GIA),³⁹ blood–brain barrier (BBB) permeation and P-glycoprotein (P-gp) substrate.³² All tested compounds except **14b** exhibit high gastrointestinal absorption, which enhance the potential for high bioavailability (Table 3). Furthermore, the three compounds are not permeable of BBB, which is expected to have a lower incidence of adverse effect on the central nervous system (CNS) (Table 3).

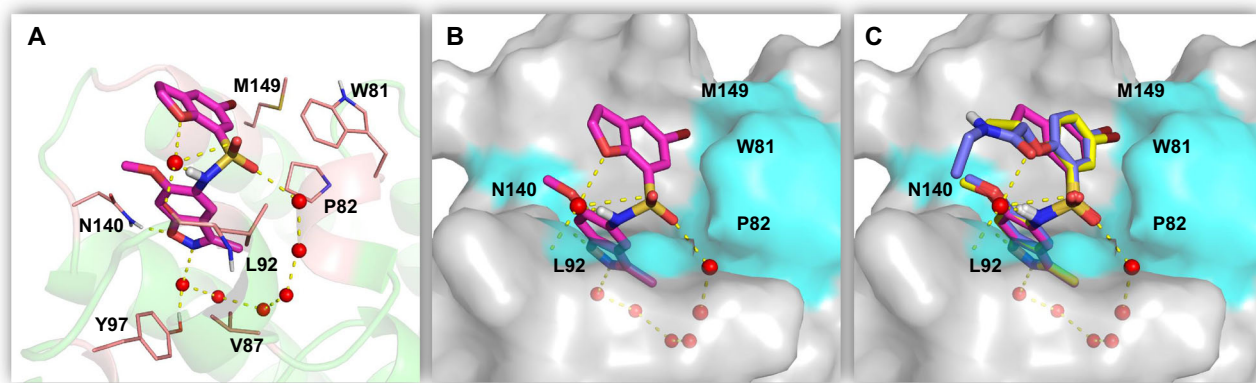


Figure 3. (a) Molecular docking of compound **13f** (magenta stick) in BRD4(1) (PDB code 5Y8Y; protein, light green ribbon; key residues, pink thin sticks; water molecules, red spheres). The isoxazole moiety forms two H-bonds (yellow dashed lines) to Asn140 and a conserved water molecule. (b) Molecular docking of compound **13f** (magenta stick) in BRD4(1) (PDB code 5Y8Y; protein, grey surface; key residues, cyan surface; water molecules, red spheres). The 3-methylbenzo[*d*]isoxazole moiety of **13f** resides in the binding pocket. (c) Overlaying the docked structures of compound **13a**, **14b** and **13f** in BRD4(1). Structures were prepared using the PyMOL program.

Table 2. *In silico* predictions of the drug-likeness and structural alerts.

No.	Lipinski violations	Ghose violations	Egan violations	Muegge violations	Veber violations	Bioavailability Score
13a	0	0	0	0	0	0.55
14b	0	1	0	0	0	0.55
13f	0	0	0	0	0	0.55

Table 3. *In silico* pharmacokinetics and medicinal chemistry friendliness parameters calculated by SwissADME^a.

Compd.	Drug-likeness filters			Structural alerts	
	GI absorption	BBB permeation	P-gp substrate	PAINS	Brenk
13a	High	No	No	0 alert	0 alert
14b	Low	No	No	0 alert	0 alert
13f	High	No	No	0 alert	0 alert

^aThe calculations were performed using online SwissADME server. GI absorption: gastrointestinal absorption; P-gp: P-glycoprotein; BBB: blood brain barrier; PAINS: pan-assay interference structures; Brenk: a structural alert reported by Brenk R *et al.*

P-glycoprotein (P-gp) is an ATP-dependent pump located on the cell membrane, which can protect cells via the efflux of invading compounds. If the drug is the substrate of P-gp, the activity of the drug will be limited *in vivo* or at the cellular level. All three compounds are not substrates of P-gp according to the parameters. Finally, the PAINS (pan-assay interference structures) and Brenk alerts were used to identify

the problematic structure in medicinal chemistry. Brenk⁴⁰ consists of 105 substructures, which may be toxic or metabolically unstable. PAINS⁴¹ can help to identify compounds with interfering substructures that have a potent response in many protein assays regardless of the specific target. It was noteworthy that none of the tested compounds triggered any alerts as predicted by the two filters.

4. Conclusions

In conclusion, a series of novel BRD4 bromodomain inhibitors bearing a benzo[d]isoxazol scaffold was designed through a structure-based drug design strategy. The facile and efficient synthetic routes were developed for the synthesis and optimization of all compounds. The SAR studies suggest a feasible direction for chemical exploration on the 2' or 3' position. Molecular docking studies revealed the binding patterns and the structural characteristics required for high affinity for the BRD4(1). The optimal inhibitor **13f** exhibited high binding affinity to BRD4(1) with a ΔT_m value of 7.8 °C and an IC_{50} of 0.21 μM . In addition, the compound **13f** displayed acceptable drug-likeness and pharmacokinetic profiles as predicted by the silico models. All the data suggest a promising starting point for further optimization of the compounds as potent BRD4 inhibitors and exploration of the biological functions.

Supplementary Information (SI)

The Figure S1, Table S1, Table S2, experimental procedures for protein expression and purification, procedures for the preparation of intermediates **9**, **11d**, **12a-b**, **12d**, and the 1H NMR and ^{13}C NMR spectra of intermediates **12c**, **12e** and the target compounds **13a-h**, **14**, and **14a-c** are given in supplementary information. Supplementary information is available at www.ias.ac.in/chemsci.

Acknowledgements

This work was partially supported by the Natural Science Foundation of Jiangsu Province (No. BK20190246) and the Natural Science Foundation of the Jiangsu Higher Education Institutions of China (No.19KJB350011). The authors would like to thank Dr. L. Zhu, National Fine Chemicals Quality Supervision and Inspection Center, for recording NMR spectra and LC-MS measurements. The authors gratefully acknowledge the technical support of docking studies and bioassays from Dr. Y. Xu at Guangzhou Institutes of Biomedicine and Health, Chinese Academy of Science.

Compliance with ethical standards

Conflict of interest The authors declare that they have no conflict of interest.

References

- Marushige K 1976 Activation of chromatin by acetylation of histone side chains *Proc. Natl. Acad. Sci. U. S. A.* **73** 3937
- Dawson M A and Kouzarides T 2012 Cancer epigenetics: from mechanism to therapy *Cell* **150** 12
- Brennan P, Filippakopoulos P and Knapp S 2012 The therapeutic potential of acetyl-lysine and methyl-lysine effector domains *Drug Discov. Today: Ther. Strategies* **9** e101
- Filippakopoulos P, Picaud S, Mangos M, Keates T, Lambert J-P, Barsyte-Lovejoy D, Felletar I, Volkmer R, Müller S, Pawson T, Gingras A-C, Arrowsmith C H and Knapp S 2012 Histone recognition and large-scale structural analysis of the human bromodomain family *Cell* **149** 214
- Zuber J, Shi J W, Wang E, Rappaport A R, Herrmann H, Sison E A, Magoon D, Qi J, Blatt K, Wunderlich M, Taylor M J, Johns C, Chicas A, Mulloy J C, Kogan S C, Brown P, Valent P, Bradner J E, Lowe S W and Vakoc C R 2011 RNAi screen identifies Brd4 as a therapeutic target in acute myeloid leukaemia *Nature* **478** 524
- Reyes-Garau D, Ribeiro L M and Roué G 2019 Pharmacological targeting of BET bromodomain proteins in acute myeloid leukemia and malignant lymphomas: From molecular characterization to clinical applications *Cancers* **11** 1483
- Dawson M A, Prinjha R K, Dittmann A, Giotopoulos G, Bantscheff M, Chan W-I, Robson S C, Chung C-W, Hopf C, Savitski M M, Huthmacher C, Gudgin E, Lugo D, Beinke S, Chapman T D, Roberts E J, Soden P E, Auger K R, Mirguet O, Doehner K, Delwel R, Burnett A K, Jeffrey P, Drewes G, Lee K, Huntly B J and Kouzarides T 2011 Inhibition of BET recruitment to chromatin as an effective treatment for MLL-fusion leukaemia *Nature* **478** 529
- Mu J, Sun P, Ma Z and Sun P 2019 BRD4 promotes tumor progression and NF- κ B/CCL2-dependent tumor-associated macrophage recruitment in GIST *Cell Death Dis.* **10** 935
- Tian Y, Wang X, Zhao S, Liao X, Younis M R, Wang S, Zhang C and Lu G 2019 JQ1-loaded polydopamine nanoplateform inhibits c-MYC/programmed cell death ligand 1 to enhance photothermal therapy for triple-negative breast cancer *ACS Appl. Mater. Inter.* **11** 46626
- Shu S K, Lin C Y, He H H, Witwicki R M, Tabassum D P, Roberts J M, Janiszewska M, Huh S J, Liang Y, Ryan J, Doherty E, Mohammed H, Guo H, Stover D G, Ekram M B, Peluffo G, Brown J, D'Santos C, Krop I E, Dillon D, McKeown M, Ott C, Qi J, Ni M, Rao P K, Duarte M, Wu S Y, Chiang C M, Anders L, Young R A, Winer E P, Letai A, Barry W T, Carroll J S, Long H W, Brown M, Liu X S, Meyer C A, Bradner J E and Polyak K 2016 Response and resistance to BET bromodomain inhibitors in triple-negative breast cancer *Nature* **529** 413
- Faivre E J, McDaniel K F, Albert D H, Mantena S R, Plotnik J P, Wilcox D, Zhang L, Bui M H, Sheppard G S, Wang L, Sehgal V, Lin X, Huang X, Lu X, Uziel T, Hessler P, Lam L T, Bellin R J, Mehta G, Fidanze S, Pratt J K, Liu D, Hasvold L A, Sun C, Panchal S C, Nicolette J J, Fossey S L, Park C H, Longenecker K, Bigelow L, Torrent M, Rosenberg S H, Kati W M and Shen Y 2020 Selective inhibition of the BD2 bromodomain of BET proteins in prostate cancer *Nature* **578** 306

12. Asangani I A, Dommeti V L, Wang X J, Malik R, Cieslik M, Yang R D, Escara-Wilke J, Wilder-Romans K, Dhanireddy S, Engelke C, Iyer M K, Jing X J, Wu Y M, Cao X H, Qin Z S, Wang S M, Feng F Y and Chinnaiyan A M 2014 Therapeutic targeting of BET bromodomain proteins in castration-resistant prostate cancer *Nature* **510** 278
13. Asangani I A, Wilder-Romans K, Dommeti V L, Krishnamurthy P M, Apel I J, Escara-Wilke J, Plymate S R, Navone N M, Wang S M, Feng F Y and Chinnaiyan A M 2016 BET bromodomain inhibitors enhance efficacy and disrupt resistance to AR antagonists in the treatment of prostate cancer *Mol. Cancer Res.* **14** 324
14. Huang M, Zeki J, Sumarsono N, Coles G L, Taylor J S, Danzer E, Bruzoni M, Hazard F K, Lacayo N J, Sakamoto K M, Dunn J C Y, Spunt S L and Chiu B 2020 Epigenetic targeting of TERT-associated gene expression signature in human neuroblastoma with TERT overexpression *Cancer Res.* **80** 1024
15. He S, Dong G, Li Y, Wu S Y, Wang W and Sheng C 2020 Potent dual BET/HDAC inhibitors for efficient treatment of pancreatic cancer *Angew. Chem. Int. Ed.* **59** 3028
16. Fehling S C, Miller A L, Garcia P L, Vance R B and Yoon K J 2020 The combination of BET and PARP inhibitors is synergistic in models of cholangiocarcinoma *Cancer Lett.* **468** 48
17. Huang B, Yang X D, Zhou M M, Ozato K and Chen L F 2009 Brd4 coactivates transcriptional activation of NF- κ B via specific binding to acetylated RelA *Mol. Cell. Biol.* **29** 1375
18. Nicodeme E, Jeffrey K L, Schaefer U, Beinke S, Dewell S, Chung C-W, Chandwani R, Marazzi I, Wilson P, Coste H, White J, Kirilovsky J, Rice C M, Lora J M, Prinjha R K, Lee K and Tarakhovskiy A 2010 Suppression of inflammation by a synthetic histone mimic *Nature* **468** 1119
19. Jiang F, Hu Q, Zhang Z, Li H, Li H, Zhang D, Li H, Ma Y, Xu J, Chen H, Cui Y, Zhi Y, Zhang Y, Xu J, Zhu J, Lu T and Chen Y 2019 Discovery of benzo[cd]indol-2(1H)-ones and pyrrolo[4,3,2-de]quinolin-2(1H)-ones as bromodomain and extra-terminal domain (BET) inhibitors with selectivity for the first bromodomain with potential high efficiency against acute gouty arthritis *J. Med. Chem.* **62** 11080
20. Filippakopoulos P, Qi J, Picaud S, Shen Y, Smith W B, Fedorov O, Morse E M, Keates T, Hickman T T, Felletar I, Philpott M, Munro S, McKeown M R, Wang Y, Christie A L, West N, Cameron M J, Schwartz B, Heightman T D, La Thangue N, French C A, Wiest O, Kung A L, Knapp S and Bradner J E 2010 Selective inhibition of BET bromodomains *Nature* **468** 1067
21. A dose escalation study to investigate the safety, pharmacokinetics (PK), pharmacodynamics (PD) and clinical activity of GSK525762 in subjects with relapsed, refractory hematologic malignancies *ClinicalTrials.gov* NCT01943851
22. Dose escalation and dose expansion study of GSK525762 in combination with androgen deprivation therapy and other agents in subjects with castrate-resistant prostate cancer *ClinicalTrials.gov* NCT03150056
23. Seal J, Lamotte Y, Donche F, Bouillot A, Mirguet O, Gellibert F, Nicodeme E, Krysa G, Kirilovsky J, Beinke S, McCleary S, Rioja I, Bamborough P, Chung C W, Gordon L, Lewis T, Walker A L, Cutler L, Lugo D, Wilson D M, Witherington J, Lee K and Prinjha R K 2012 Identification of a novel series of BET family bromodomain inhibitors: binding mode and profile of I-BET151 (GSK1210151A) *Bioorg. Med. Chem. Lett.* **22** 2968
24. Bamborough P, Diallo H, Goodacre J D, Gordon L, Lewis A, Seal J T, Wilson D M, Woodrow M D and Chung C W 2012 Fragment-based discovery of bromodomain inhibitors part 2: optimization of phenylisoxazole sulfonamides *J. Med. Chem.* **55** 587
25. Hewings D S, Fedorov O, Filippakopoulos P, Martin S, Picaud S, Tumber A, Wells C, Olcina M M, Freeman K, Gill A, Ritchie A J, Sheppard D W, Russell A J, Hammond E M, Knapp S, Brennan P E and Conway S J 2013 Optimization of 3,5-dimethylisoxazole derivatives as potent bromodomain ligands *J. Med. Chem.* **56** 3217
26. Ran X, Zhao Y J, Liu L, Bai L C, Yang C Y, Zhou B, Meagher J L, Chinnaswamy K, Stuckey J A and Wang S M 2015 Structure-based design of γ -carboline analogues as potent and specific BET bromodomain inhibitors *J. Med. Chem.* **58** 4927
27. Xue X Q, Zhang Y, Liu Z X, Song M, Xing Y L, Xiang Q P, Wang Z, Tu Z C, Zhou Y L, Ding K and Xu Y 2016 Discovery of benzo[cd]indol-2(1H)-ones as potent and specific BET bromodomain inhibitors: structure-based virtual screening, optimization, and biological evaluation *J. Med. Chem.* **59** 1565
28. Zhang M, Zhang Y, Song M, Xue X, Wang J, Wang C, Zhang C, Li C, Xiang Q, Zou L, Wu X, Wu C, Dong B, Xue W, Zhou Y, Chen H, Wu D, Ding K and Xu Y 2018 Structure-based discovery and optimization of benzo[d]isoxazole derivatives as potent and selective BET inhibitors for potential treatment of castration-resistant prostate cancer (CRPC) *J. Med. Chem.* **61** 3037
29. Albaster R J, Cottrell I F, Marley H and Wright S H B 1988 The synthesis of 5-substituted 2,3-dihydrobenzofurans *Synthesis-Stuttgart* 950
30. Zhang Z, Zhu M and Tang W 2009 Metabolite identification and profiling in drug design: current practice and future directions *Curr. Pharm. Des.* **15** 2220
31. Zhang Z and Tang W 2018 Drug metabolism in drug discovery and development *Acta Pharm. Sin. B* **8** 721
32. Daina A, Michielin O and Zoete V 2017 SwissADME: a free web tool to evaluate pharmacokinetics, drug-likeness and medicinal chemistry friendliness of small molecules *Sci. Rep.* **7** 42717
33. Lipinski C A, Lombardo F, Dominy B W and Feeney P J 1997 Experimental and computational approaches to estimate solubility and permeability in drug discovery and development settings *Adv. Drug Deliver. Rev.* **23** 3
34. Ghose A K, Viswanadhan V N and Wendoloski J J 1999 A knowledge-based approach in designing combinatorial or medicinal chemistry libraries for drug discovery. 1. A qualitative and quantitative characterization of known drug databases *J. Comb. Chem.* **1** 55

35. Egan W J, Merz K M and Baldwin J J 2000 Prediction of drug absorption using multivariate statistics *J. Med. Chem.* **43** 3867
36. Muegge I, Heald S L and Brittelli D 2001 Simple selection criteria for drug-like chemical matter *J. Med. Chem.* **44** 1841
37. Veber D F, Johnson S R, Cheng H Y, Smith B R, Ward K W and Kopple K D 2002 Molecular properties that influence the oral bioavailability of drug candidates *J. Med. Chem.* **45** 2615.
38. Martin Y C 2005 A bioavailability score *J. Med. Chem.* **48** 3164
39. Daina A and Zoete V 2016 A BOILED-Egg to predict gastrointestinal absorption and brain penetration of small molecules *ChemMedChem* **11** 1117
40. Brenk R, Schipani A, James D, Krasowski A, Gilbert I H, Frearson J and Wyatt P G 2008 Lessons learnt from assembling screening libraries for drug discovery for neglected diseases *ChemMedChem* **3** 435
41. Baell J B and Holloway G A 2010 New substructure filters for removal of pan assay interference compounds (PAINS) from screening libraries and for their exclusion in bioassays *J. Med. Chem.* **53** 2719